

# Evidence of quantum criticality in the doped Haldane system $\text{Y}_2\text{BaNiO}_5$

C. Payen, E. Janod, K. Schoumacker

*Institut des Matériaux Jean Rouxel, Université de Nantes-CNRS,  
44322 Nantes  
Cedex 3, France*

C. D. Batista, K. Hallberg, A. A. Aligia

*Centro Atómico Bariloche and Instituto Balseiro,  
Comisión Nacional de Energía Atómica 8400 S.C. de Bariloche,  
Argentina*

(November 20, 2018)

Experimental bulk susceptibility  $\chi(T)$  and magnetization  $M(H, T)$  of the  $S=1$  Haldane chain system doped with nonmagnetic impurities,  $\text{Y}_2\text{BaNi}_{1-x}\text{Zn}_x\text{O}_5$  ( $x \leq 0.08$ ), are analyzed. A numerical calculation for the low-energy spectrum of non-interacting open segments describes very well experimental data above 4 K. Below 4 K, we observe power-law behaviors,  $\chi(T) \sim T^{-\alpha}$  and  $M(H, T) \sim T^{1-\alpha} f_\alpha(H/T)$ , with  $\alpha$  ( $< 1$ ) depending on the doping concentration  $x$ . This observation suggests the appearance of a gapless quantum phase due to a broad distribution of effective couplings between the dilution-induced moments.

75.10.Jm, 75.45.+j, 75.40.Cx, 75.40.Mg

The past two decades have seen a resurgence of interest devoted to macroscopic quantum phenomena in Heisenberg antiferromagnets (HAF). A current issue in this field concerns the interplay between quantum spin fluctuations and quenched (i.e., time-independent) disorder in one dimension (1D) [1]. A simple nontrivial model to address this issue is the 1D-HAF with spins  $S = 1$ , which has a Haldane gap  $\Delta \approx 0.4J$  and a short correlation length  $\xi \approx 6$  in its spin-liquid ground state ( $J$  is the nearest-neighbor exchange parameter) [2,3]. In this system, the disorder in the form of site depletion leads to interesting quantum phenomena due to the creation of two effective  $S = 1/2$  spins on the opposite edges of a segment, near the vacancies [4,5]. The inclusion of weak magnetic bonds across the spin-vacancies induces bond disorder and causes departure from simple finite-size behaviors. In this case, some recent theoretical works, for the  $S = 1$  chain with variable nonmagnetic doping, found a quantum (zero-temperature) phase transition from the Haldane phase to a 1D random-singlet (RS) phase in which effective spins are coupled into singlets over all length scales [6,7]. On the experimental side, however, this problem has been very little explored from the point of view of quantum criticality. While it is known that some  $S = 1$  diluted compounds can sustain paramagnetism down to low temperature, most of the existing experimental studies aimed to confirm the existence of  $S = 1/2$  end-chain states or to reveal the internal structure of these end states [4,8]. A noticeable exception is the recent observation of a 3D long-range order (LRO) caused by nonmagnetic doping in  $\text{PbNi}_2\text{V}_2\text{O}_8$  [9]. This Haldane system shows, however, substantial interchain interactions, so it is almost critical towards the formation of a LRO in the absence of intentional disorder.

In this work, we examine the effects of nonmagnetic

doping on the bulk magnetic responses in the  $S = 1$  quasi-1D-HAF  $\text{Y}_2\text{BaNiO}_5$ . We chose this well characterized system because of the rather high value of its main energy scale,  $J \approx 280$  K, and the very small value of the interchain coupling,  $|J_\perp/J| < 10^{-3}$  [10]. Furthermore, it has a simple orthorhombic crystal structure [11] and a small single-ion anisotropy ( $D/J \approx -0.04$ ,  $E/J \approx -0.01$ ) [10]. A weak nonmagnetic doping in  $\text{Y}_2\text{BaNiO}_5$ , which is realized by substituting  $\text{Zn}^{2+}$  or  $\text{Mg}^{2+}$  ions for the  $S = 1$   $\text{Ni}^{2+}$  ions, yields new magnetic states below the Haldane gap ( $\Delta \approx 100$  K) with no sign of LRO down to very low temperature [12–14]. Recently, the low-temperature specific heat of  $\text{Y}_2\text{BaNi}_{1-x}\text{Zn}_x\text{O}_5$  ( $x = 0.04$ ) and the ESR spectra of a series of Mg-doped compounds have been quantitatively explained by an effective model which describes the low-energy spectrum of non-interacting open  $S = 1$  chains [15,16]. These results and the recent NMR experiments in Ref. 8 are strong indications of the existence of  $S = 1/2$  end-chain states. In the present work, we analyze new susceptibility and magnetization data for  $\text{Y}_2\text{BaNi}_{1-x}\text{Zn}_x\text{O}_5$  with  $0.04 \leq x \leq 0.08$ . Above 4 K, the simple model of non-interacting segments used in Refs. [15,16] describes the data very well. However, at very low temperature we observe a new regime with divergent power law behavior, which is similar to that observed in some doped semiconductors [17]. Our results support the existence of a zero-temperature gapless phase due to randomness in the effective bond distribution that is reinforced by the interchain interactions. The low-energy effective model for this phase resembles a 2D or 3D RS state.

Figure 1 shows the linear susceptibilities,  $\chi(T)$ , measured with a commercial SQUID magnetometer for a series of polycrystalline samples of  $\text{Y}_2\text{BaNi}_{1-x}\text{Zn}_x\text{O}_5$  ( $x = 0, 0.04, 0.06$  and  $0.08$ ) that were prepared through

standard solid-state reactions [11]. The results obtained for the nominally pure sample compare well with those in the published literature [12]. At low temperatures,  $\chi(T)$  is well fitted by the sum of a  $T$ -independent term  $\chi_0$ , a Curie law and a thermally activated term with  $\Delta \approx 100$  K (see Fig.1). The sum of the activated part and the constant  $\chi_0 \approx 10^{-4}$  cm<sup>3</sup>/mol is negligible below 15 K. The low-temperature susceptibility (below 10-15 K) for  $x = 0$  is mainly due to the Curie contribution that corresponds to 1.4 percent of free  $S = 1/2$  spins per formula unit. This Curie behavior can be interpreted as coming from natural crystal defects and a weak excess oxygen. The main effect of the intentional nonmagnetic dilution is to increase drastically the low-temperature upturn in  $\chi(T)$ , as is evident from Fig. 1. This indicates the existence of paramagnetic moments whose amount is related to the doping concentration. The behavior of  $\chi(T)$  is however qualitatively the same, regardless of the level of dilution. The data for the doped compounds were first analyzed with a modified Curie-Weiss law,  $\chi(T) = \chi_0 + C/(T - \theta)$ , between 1.9 and 15 K. A small phenomenological  $\theta \approx 0.6$  K was required to describe the data. The dependence of the Curie constant  $C$  as a function of the Zn doping is shown in the inset of Fig. 1. At low doping, the observed  $C$  value is that for two  $S = 1/2$  spins per nonmagnetic impurity. At high  $x$ , however, the Curie constant should be that for one half of a spin-1 per Zn since a short segment with an odd (even) number of spins behaves as a  $S = 1$  ( $S = 0$ ) 'molecular' entity at low temperature and the number of odd chains is half the total number of chains. This tendency seems to be observed (see Fig. 1). We have also measured the magnetization,  $M(H, T)$ , for applied field up to 5 T. For all samples,  $M(H, T) - \chi_0 H$  shows a non-Brillouin behavior and is smaller than twice the Brillouin function for one  $S = 1/2$  spin per Zn.

To go further in our analysis, we have compared the experimental data with a theoretical model based on the picture of non-interacting segments, as described hereafter. The energy spectrum of finite segments described by the  $S = 1$  Heisenberg Hamiltonian is characterized by four low-energy states, a singlet and a triplet [3]. It corresponds to the existence of a coupling between the two  $S = 1/2$  edge spins, which may be AF or ferromagnetic (F). The energy difference among these levels decreases exponentially with the length of the chain  $N$ , as  $(-1)^N e^{-N/\xi}$ , and already for chains of a few lattice sites, these four states are separated from the rest of the spectrum by an energy of the order of the Haldane gap [3]. Therefore at temperature  $T$  and magnetic energies  $\mu_B H$  much lower than the Haldane gap, the magnetic and thermal properties of a system composed of segments of several lengths are completely described by the energy of these four states and the matrix elements of the magnetization operator in this reduced subspace. We have calculated these quantities using the Density Matrix Renormalization Group (DMRG) method. The resulting

Hamiltonian which describes the low-energy properties of a segment including the triplet  $|1, S_z\rangle$  and the singlet state  $|0\rangle$  is:

$$H_{eff} = E_0(N) + (J\alpha(N) + D\beta(N)) |0\rangle \langle 0| + D\gamma(N) S_z^2 + E\gamma(N)(S_x^2 - S_y^2) - \mu_B \sum_{\nu\alpha} H^\alpha g^{\alpha\nu} S_t^\nu, \quad (1)$$

where  $E_0(N)$ ,  $\alpha(N)$ ,  $\beta(N)$  and  $\gamma(N)$  are functions of the chain length  $N$  (determined from the DMRG data). The validity of the last term has been verified explicitly by calculating the matrix elements of  $S_t^+$ , and  $S_t^-$  for all chains. The magnetic moment operator is  $-\nabla_H H_{eff}$ , and to compare with experiments in polycrystalline samples, we have averaged its expectation value over all possible orientations of the crystal. Also, a distribution of chain segments corresponding to a random distribution of defects was assumed [16]. Figure 2 shows the comparison between the measured  $\chi(T)T$  products for  $T < 12$  K and the numerical solution. The adjustable parameters in the calculations were the doping  $x$  and  $\chi_0$ . All the other parameters were held fixed at the values deduced from previous works [10,16]:  $J = 280$  K,  $D/J = -0.039$ ,  $E/J = -0.013$ ,  $g_x = g_y = 2.17$  and  $g_z = 2.20$ . The fitted values of  $x$  ( $x = 0.041, 0.060$  and  $0.074$ ) are close to the nominal concentrations, and the fitted  $\chi_0$  remains in the expected range ( $\chi_0 = 1.0 \times 10^{-4}$  to  $1.9 \times 10^{-4}$  cm<sup>3</sup>/Ba-mol). Taking into account that uncertainties in the above parameters might affect the theoretical curve, the success of the anisotropic model of non-interacting segments to explain the data above 4 K is remarkable. Note that for the cases with nominal concentration of Zn  $x = 0.06$  and  $x = 0.08$ , a decrease of the order of 5% or less in the actual  $x$  used, would improve considerably the fitting above 5 K, but increase the differences between theory and experiment in the low-temperature part. Instead, because of the different rate of change of both curves, it is not possible to obtain a good fit for  $T < 4$  K by small changes of  $x$  or other parameters. A good agreement between the experimental magnetization ( $M(H, T) - \chi_0 H$ ) and the numerical data above 4 K (not shown) is also achieved using the parameters required to describe the susceptibility data. This noticeable agreement confirms the existence of the  $S = 1/2$  end-chain excitations. Note that an accurate description of the experimental data needs to consider both, a random distribution of defects [16] and the effect of the single-ion anisotropy [15,16], which is stronger for shorter segments.

However, below 4 K, the experimental data deviates from the predictions of the above described model. This is seen in Fig. 2 for the susceptibility. It is also observed for our magnetization data  $M(H, T) - \chi_0 H$ . In previous studies of specific heat and electron spin resonance, while excellent agreement was obtained above 4 K, a discrepancy was also found below this temperature and interpreted as the onset of interchain interac-

tions not taken into account in this model [15,16]. An analysis of the susceptibility shows that, in the vicinity of 4 K, there is a crossover to a sub-Curie power law regime,  $[\chi(T) - \chi_0] \sim T^{-\alpha}$  with  $\alpha = 0.83, 0.79$  and  $0.76$  for  $x = 0.04, 0.06$  and  $0.08$ , respectively (see Fig. 3). The susceptibility data for the Mg-doped compound  $\text{Y}_2\text{BaNi}_{0.959}\text{Mg}_{0.041}\text{O}_5$  in Ref. [14] also obey a power-law form with  $\alpha = 0.73$  (see Fig. 3). This behavior, which cannot be reproduced by the model of non-interacting segments, is reminiscent of some random exchange Heisenberg systems for which the AF couplings between nearest-neighbor  $S = 1/2$  spins are random in their magnitude, such as insulating phosphorous-doped silicon (Si:P) [17]. Bhatt and Lee have proposed a theoretical method to explain the properties of Si:P [18]. Within this approach, the spin pairs with the strongest AF bonds freeze into inert singlets, leaving behind a new ensemble of active spins with a renormalized distribution of exchange, and the quantum fluctuations drive the whole system into a ground state consisting of random local singlets (RS phase). The behavior of the susceptibility,  $\chi(T) \sim T^{-\alpha}$  with  $\alpha < 1$ , follows from a divergent power-law distribution of the renormalized exchange,  $P(J) \sim J^{-\alpha}$ . A scaling of the magnetization has been also predicted and experimentally observed [17],  $M(H, T)/T^{1-\alpha} = f_\alpha(H/T)$ . A similar scaling is, in fact, very well obeyed by our data below (but not above) 4 K using the  $\alpha$  exponents determined from the susceptibility. Fig. 3 shows a plot of  $(M(H, T) - \chi_0 H)/T^{1-\alpha}$  versus  $H/T$  for each of the three samples studied. All the data for each sample, for different magnetic fields and temperatures, lie on a single scaling curve, which is however different from the expression of  $f_\alpha(H/T)$  calculated on the basis of the Bhatt and Lee's solution for Si:P [17]. This is illustrated in Fig. 3 for  $\text{Y}_2\text{BaNi}_{0.94}\text{Zn}_{0.06}\text{O}_5$ .

These power law behaviors show that the picture of the ideal 1D anisotropic Heisenberg non-interacting chain breaks down below 4 K, and that additional interactions play a role. From simple arguments based on perturbation theory, one expects that the dominant inter-chain interaction is a coupling  $J_{\perp b}$  between  $S = 1$  spins lying in nearest-neighbor chains along the  $b$  direction, perpendicular to the chain axis  $a$ . A calculation using the cell perturbation method gives  $J_{\perp b} \approx 0.2$  K [19]. This interaction should be at least an order of magnitude larger than that between two spins on the same atomic chain, with a Zn atom in between. As discussed in more detail in Ref. [15,19]  $J_{\perp b}$  induces an effective interaction  $J'$  between  $S = 1/2$  end-states of neighboring chains along the  $b$  direction, the magnitude and sign of which depends on the detailed position of the defects. The maximum absolute value of  $J'$  is of the order of  $10J_{\perp b}$  and it should decay exponentially with the distance along the chain between the defects. Since the interaction between  $S = 1/2$  defects lying in different  $ab$  planes is expected to be at least an order of magnitude smaller, the physics in the

range  $0.1 \text{ K} < T < 4 \text{ K}$  seems to correspond to a 2D array of  $S = 1/2$  spins, with random F and AF interactions coming from exponentially decaying intra- and interchain couplings.

In agreement with this, the spin glass behavior observed below 3 K in Ca doped systems  $\text{Y}_{2-y}\text{Ca}_y\text{BaNiO}_5$  indicates a dimensionality higher than one in the system at low temperature [14,19]. For a 2D or 3D  $S = 1/2$  model with random AF interactions, Bhatt and Lee obtained a power law behavior with  $\alpha (< 1)$  depending on the doping concentration [18]. This result is consistent with our observations but, as mentioned above, we obtain a different scaling function for the magnetization. This might be due to the presence of effective F coupling in  $\text{Y}_2\text{BaNi}_{1-x}\text{Zn}_x\text{O}_5$ . Our results can also be compared to a recent theoretical work in which the spin-1 chain with an AF coupling across nonmagnetic impurities is mapped onto a bond disordered spin-1/2 chain [6]. Within this 1D approach, the Haldane state is found to be stable to weak dilution. For sufficiently strong randomness, however, the system flows towards a 1D RS phase with diverging correlation length. In this gapless phase, the form of the low energy asymptotic behavior of  $\chi(T)$  is independent of the level of the disorder,  $\chi(T) \sim 1/(T \ln^2 T)$ . In the Haldane phase, there is a Griffiths gapless region where  $\chi(T)$  varies as  $T^{-\alpha}$  with  $\alpha (< 1)$  which is dependent of the details of the randomness. It is unclear however whether a similar physics should be valid or not when interchain coupling is turned on [20]. Furthermore, the form of the asymptotic behavior of  $\chi(T)$  is not known for a 2D or 3D RS phase [1]. If there were no interchain coupling  $J_{\perp}$ , the low-energy model for  $\text{Y}_2\text{BaNi}_{1-x}\text{Zn}_x\text{O}_5$  with  $0.04 \leq x \leq 0.08$  would be the 1D RS phase depicted in Ref. [6] since the bond across a Zn is expected to be much weaker than the average coupling between the  $S = 1/2$  edges within a segment [15]. From our observations, it is tempting to say that the  $H/T$  variable in the scaling of  $M(H, T)$  indicates a  $T_c = 0$  critical point and that  $\text{Y}_2\text{BaNi}_{1-x}\text{Zn}_x\text{O}_5$  has a quantum critical ground state even for the smallest doping  $x = 0.04$ . From the theoretical point of view, the detailed explanation of the observed power-law behaviors remains open.

Interestingly, a similar singular behavior has been disclosed for two  $S = 1$  1D-HAF compounds, namely  $\text{AgVP}_2\text{S}_6$  and NENP, on nominally pure samples [20]. A broad distribution of couplings between the dilution-induced moments and quantum fluctuations drives  $\text{Y}_2\text{BaNi}_{1-x}\text{Zn}_x\text{O}_5$ , and perhaps other real systems as well, towards a novel ground state which resembles a random valence bond state. This is in contrast with the LRO observed in  $\text{PbNi}_2\text{V}_2\text{O}_8$  [9]. Therefore there is no universal behavior under nonmagnetic doping in real  $S = 1$  1D-HAF substances. Details of the topology of the magnetic interaction lattice are probably crucial in determining the way the Haldane phase is destabilized by the quenched disorder.

K.H. and C.D.B. are supported by CONICET, Argentina. A.A.A. is partially supported by CONICET. C.P. is partially supported by the 'Institut Universitaire de France'. C.P. thanks H. Mutka for helpful discussions and continued support. K. H. is grateful to the Physics Department of the University of Buenos Aires for the hospitality during this work. This work was supported by PICT 03-00121-02153 of ANPCyT and PIP 4952/96 of CONICET.

- 
- [1] D. S. Fisher, Phys. Rev. B **50**, 3799 (1994).
  - [2] I. Affleck, J. Phys.: Condens. Matter **1**, 3047 (1989).
  - [3] T. Kennedy, J. Phys.: Condens. Matter **2**, 5737 (1990).
  - [4] S.H. Glarum, S. Geschwind, K. M. Lee, M. L. Kaplan and J. Michel, Phys. Rev. Lett. **67**, 1614 (1991).
  - [5] S. Miyashita and S. Yamamoto, Phys. Rev. B **48**, 913 (1993).
  - [6] R.A. Hyman and K. Yang, Phys. Rev. Lett. **78**, 1783 (1997).
  - [7] C. Monthus, O. Golinelli and T. Jolicoeur, Phys. Rev. Lett. **79**, 3254 (1997).
  - [8] F. Tedoldi, R. Santachiara and M. Horvatic, Phys. Rev. Lett. **83**, 412 (1999).
  - [9] Y. Uchiyama, Y. Sasago, I. Tsukuda, K. Uchinokura, A. Zheludev, T. Hayashi, N. Miura and P. Boni, Phys. Rev. Lett. **83**, 632 (1999).
  - [10] T. Sakaguchi, K. Kakurai, T. Yokoo and J. Akimitsu, J. Phys. Soc. Jpn. **65**, 3025 (1996).
  - [11] D.J. Buttrey, J.D. Sullivan and A.L. Rheingold, J. Solid State Chem. **88**, 291 (1990).
  - [12] B. Batlogg, S-W. Cheong and L.W. Rupp Jr, Physica B **194-196**, 173 (1994).
  - [13] J.F. DiTusa, S-W. Cheong, J.-H. Park, G. Aeppli, C. Broholm and C.T. Chen, Phys. Rev. Lett. **73**, 1857 (1994).
  - [14] K. Kojima, A. Keren, L.P. Lee, G.M. Luke, B. Namuchi, W.D. Wu, Y.J. Uemura, K. Kiyono, S. Miyasaka, H. Takagi and S. Uchida, Phys. Rev. Lett. **74**, 3471 (1995).
  - [15] C.D. Batista, K. Hallberg and A.A. Aligia, Phys. Rev. B **58**, 9248 (1998).
  - [16] C.D. Batista, K. Hallberg and A.A. Aligia, Phys. Rev. B **60**, R12553 (1999).
  - [17] R.N. Bhatt, Physica Scripta **T14**, 7 (1986).
  - [18] R.N. Bhatt and P.A. Lee, Phys. Rev. Lett. **48**, 344 (1982).
  - [19] C.D. Batista, A.A. Aligia and J. Eroles, Europhys. Lett. **43**, 71 (1998).
  - [20] M. Fabrizio and R. Melin, J. Phys.: Condens. Matter **9**, 10429 (1997).
  - [21] H. Mutka, C. Payen, P. Molinie, Solid State Commun. **85**, 597 (1993).

FIG. 1. Magnetic susceptibility versus temperature,  $\chi(T)$ , for  $\text{Y}_2\text{BaNi}_{1-x}\text{Zn}_x\text{O}_5$  ( $0 \leq x \leq 0.08$ ). The solid line is a fit for  $x=0$  with  $\chi = \chi_0 + C/(T-\theta) + A(\Delta/T)^{1/2}e^{-\Delta/T}$ . The sum of the first and third terms is shown as a dashed line. Inset: the doping dependence of  $C$  as described in the text. Data from Ref. [12] (open circle) and [14] (square) for Mg-doped  $\text{Y}_2\text{BaNiO}_5$  are included for comparison. Solid and dashed lines show the result assuming that one impurity creates two free  $S=1/2$  spins and one half of a  $S=1$  spin, respectively.

FIG. 2.  $\chi T$  versus  $T$  plot for  $\text{Y}_2\text{BaNi}_{1-x}\text{Zn}_x\text{O}_5$  ( $0.04 \leq x \leq 0.08$ ) in the range 1.9-12 K. Errors bars are of the order of the sizes of the symbols. The solid lines show the best fits with our numerical solution, as described in the text. The dashed and dotted lines are for the two free  $S=1/2$  spins prediction and a numerical calculation neglecting the single-ion anisotropy, respectively, for  $x=0.06$ .

FIG. 3. Power-law scaling of the magnetization,  $[M(H, T) - \chi_0]/T^{1-\alpha} = f_\alpha(H/T)$ , for  $\text{Y}_2\text{BaNi}_{1-x}\text{Zn}_x\text{O}_5$  ( $0.04 \leq x \leq 0.08$ ) in the range 1.9-4 K with data taken every 0.1K. The values of  $\alpha$  are determined from the susceptibilities. The solid line is the theoretical expression of  $f_\alpha(H/T)$  from Ref. [17] for  $x=0.06$ . Inset: Double-logarithmic plot of  $[\chi(T) - \chi_0]T$  versus  $T$  for  $\text{Y}_2\text{BaNi}_{1-x}\text{Zn}_x\text{O}_5$ . Data for  $\text{Y}_2\text{BaNi}_{0.959}\text{Mg}_{0.041}\text{O}_5$  in Ref. [14] are shown as open diamonds.

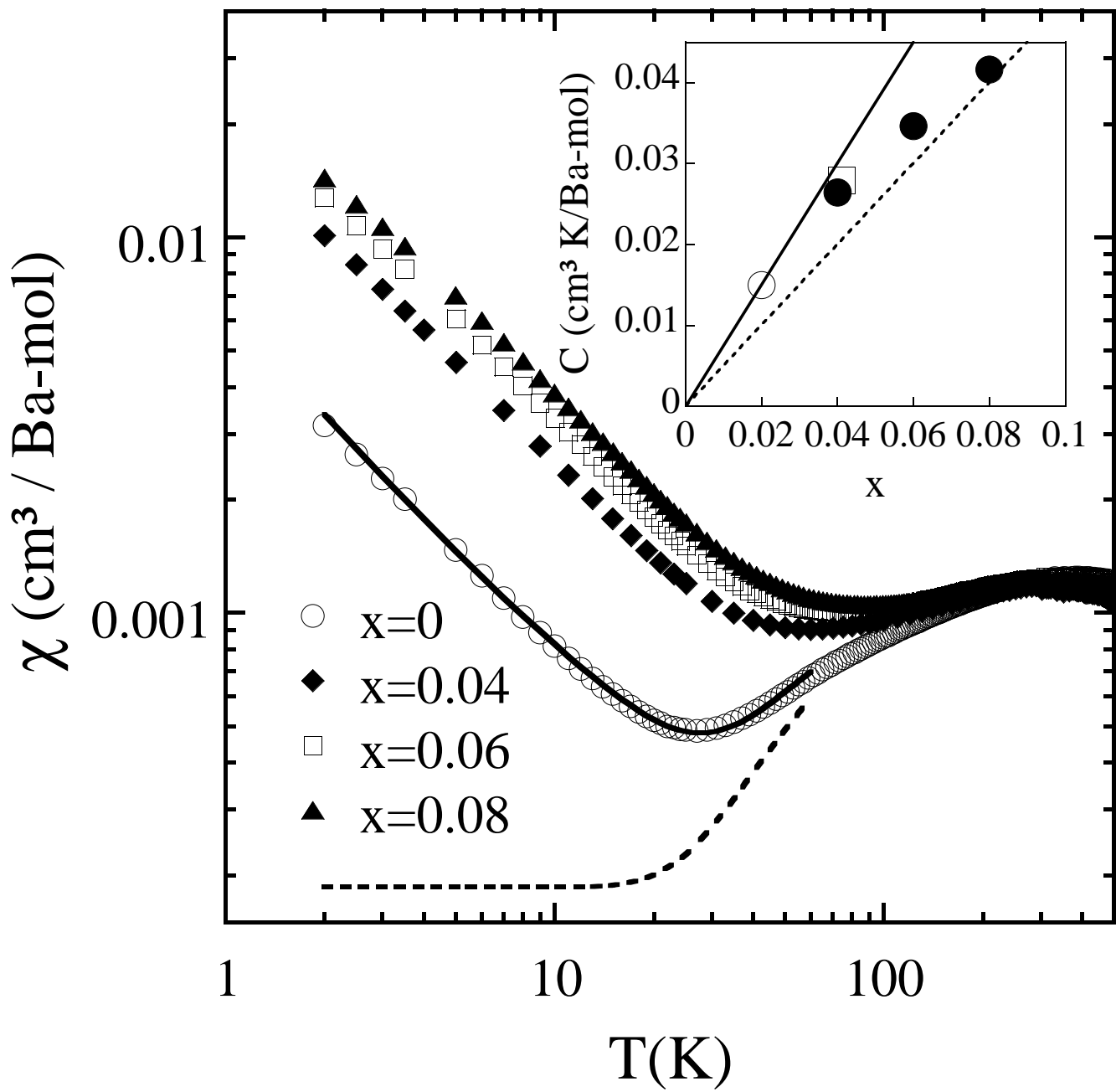


Figure 1

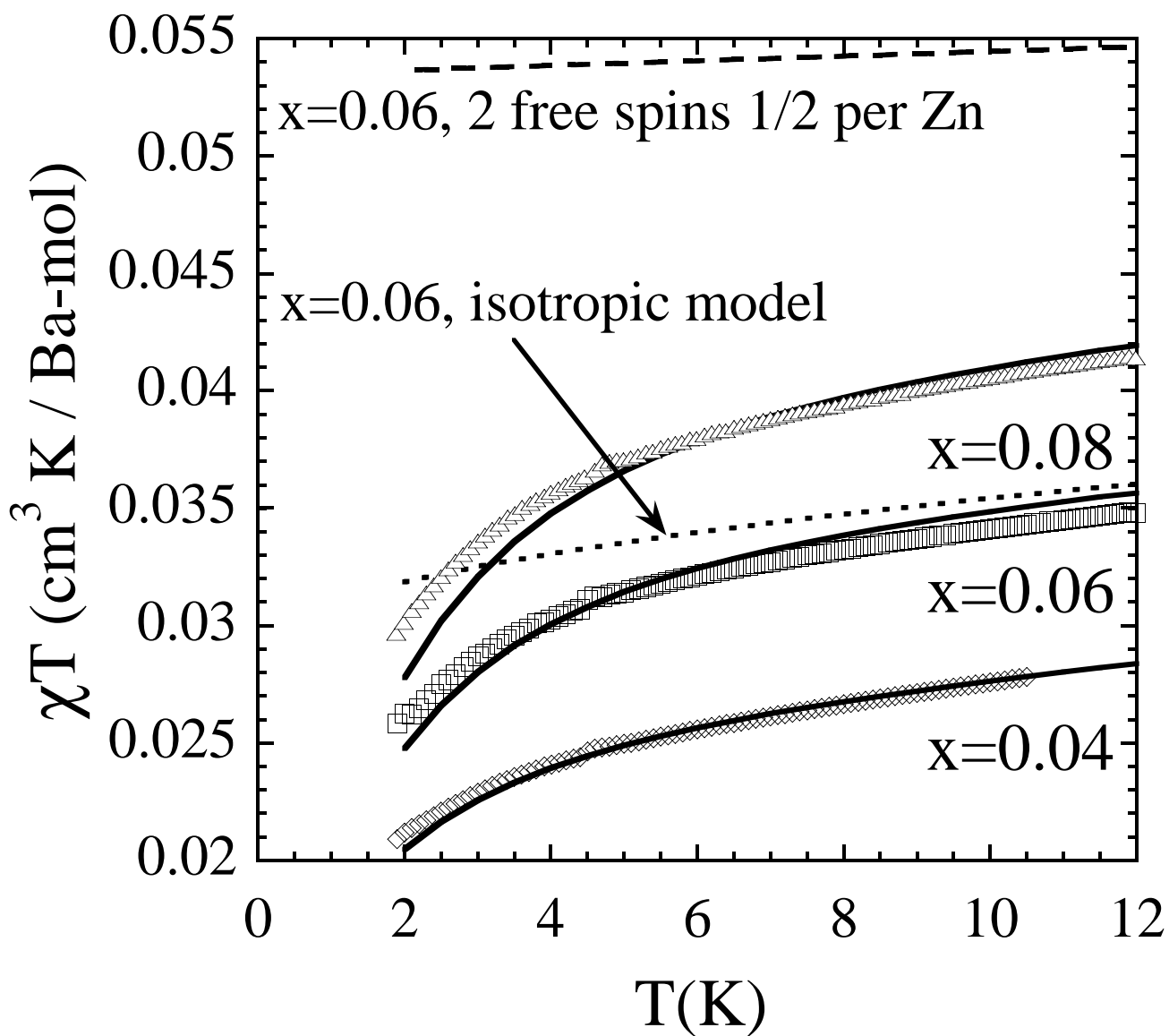


Figure 2

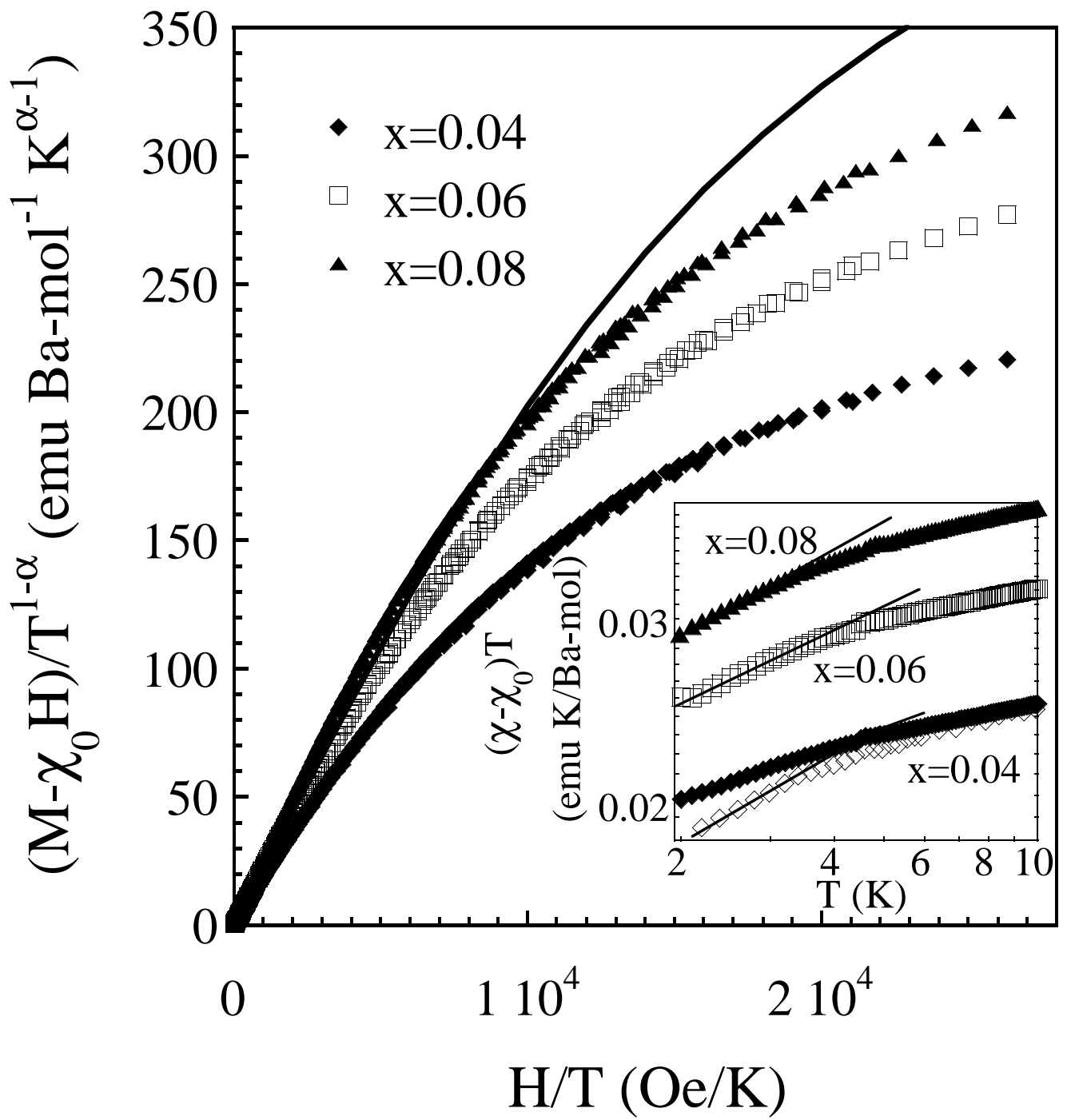


Figure 3